Hyperfine Interactions (2020) 241:6
https://doi.org/10.1007/s10751-019-1681-9

Magnetic property and ^{57}Fe Mössbauer analysis of dilute Fe and Nb codoped $SrTiO_{3-\delta}$(STO) perovskites

Kiyoshi Nomura[1,2] · Shuhei Yamakawa[2] · Miki Kasari[2] · Yuya Koike[2] · Akio Nakanishi[3] · Shiro Kubuki[1] · Atsushi Okazawa[4]

Published online: 10 December 2019

Abstract
Dilute Fe and Nb codoped $SrTiO_{3-\delta}$ (STO) perovskites were prepared by a complex formation and thermal decomposition method. The structure, magnetization properties and chemical states of Fe and Nb codoped STO perovskites were characterized by XRD, VSM and Mössbauer spectrometry. Mössbauer spectra of ^{57}Fe and Nb codoped STO perovskites consist of paramagnetic doublet and magnetic relaxation components. The 1% Fe + 5% Nb codoped STO sample showed the smallest lattice constant and the largest ferromagnetism among 0.5–4% Fe + 5% Nb codoped STO perovskites. The most distortion of cubic STO lattice and the largest magnetic relaxation in Mössbauer spectrum were observed for the 0.5% Fe and 5% Nb codoped STO perovskite. It is considered that diluted magnetism in this system is related with the deformation of cubic structure due to defects.

Keywords Diluted magnetism · Perovskite oxide · Fe and Nb doped $SrTiO_3$ · Mössbauer analysis

This article is part of the Topical Collection *Proceedings of the International Conference on the Applications of the Mössbauer Effect (ICAME2019), 1-6 September 2019, Dalian, China*
Edited by Tao Zhang, Junhu Wang and Xiaodong Wang

✉ Kiyoshi Nomura
dqf10204@nifty.com

[1] Radio Isotopes Center, Tokyo Metropolitan University, Minami-osawa 1-1, Hachioji, Tokyo 192-0364, Japan

[2] Faculty of Science and Engineering, Meiji University, Higashi-mita 1-1-1, Tama-ku, Kawasaki, Kanagawa 214-8571, Japan

[3] Department of Physics, Shiga University of Medical Science, Tukimiwa 1-1, Seta, Shiga 520-2192, Japan

[4] Graduate School of Arts and Sciences, The University of Tokyo, Komaba 3-8-1, Megro-ku, Tokyo 153-8902, Japan

1 Introduction

Diluted magnetic oxide semiconductors doped with magnetic ions are one of the candidate materials for spintronic applications. Magnetic ion doping into wide band gap semiconductors such as SnO_2 [1], TiO_2 [2], and ZnO [3] have been studied. Uniform oxides doped with dilute magnetic ions are expected to improve magnetic and semiconductor properties at room temperature. Perovskite oxides are also expected to obtain similar characteristics by doping dilute magnetic ions. The band gap of cubic $SrTiO_3$ (STO) perovskite is as wide as 3.2 eV, which is the same as TiO_2. $SrFeO_3$ is a cubic perovskite and is converted to an orthorhombic phase with many oxygen defects. A. S. Kumar et al. [4] reported the magnetic and ferroelectric properties of Fe doped $SrTi_{1-x}Fe_xO_{3-\delta}$films with doping rates (x) from 0.2 to 0.9. They have shown that ferroelectricity is induced by modifying the crystal structure from simple cubic to tetragonal. A distorted perovskite structure with tolerance factors less than 1 can induce polarization. Similarly, the cubic symmetry in $SrTiO_3$ can be reduced by reducing oxygen. The annealing effect on magnetic properties of Fe-doped $SrTiO_3$ nanopowders prepared by hydrothermal method was studied [5]. The magnetic properties of $SrTiO_3$ implanted with 40 keV Fe ions at the fluencies between 0.5×10^{17} and 1.5×10^{17} ion/cm^2 were investigated [6], and ferromagnetic hysteresis loop was observed in Fe implanted $SrTiO_3$ at low temperatures.

On the other hand, it is known that the electrical properties of $SrTiO_3$ ceramics were increased by doping Nb^{5+}. Maximum electrical conductivity (ca. 55 S cm^{-1} at 650 °C) has been observed for the $SrTi_{0.98}Nb_{0.02}O_{3-\delta}$ sample [7]. The resistivity, carrier concentration and mobility of the Nb doped STO thin film are 3.6×10^{-4} Ω cm, 2.8×10^{21} cm^{-3} and 12.7 cm^2/V s, respectively [8]. Furthermore, (Nb, N) or (Nb, Ru) codoping effects for $SrTiO_3$ have been studied from viewpoints of enhancement of visible light photocatalytic activity of $SrTiO_3$: a hybrid density functional study [9]. Surface magnetism of strontium titanite was reported by J. M. D. Coey et al. [10].

However, $SrTiO_{3-\delta}$ doped with dilute Fe (< 10%) and Nb (several %) have not been studied well. $SrTiO_{3-\delta}$ are expected to improve the magnetic and electric properties by codoping dilute Fe^{3+} and Nb^{5+} ions. We report here the magnetic properties and ^{57}Fe Mössbauer analyses of dilute Fe and Nb codoped $SrTiO_{3-\delta}$, $SrTi_{0.95-x}Nb_{0.05}Fe_xO_{3-\delta}$(x= 0.005 to 0.04), prepared by a complex formation and thermal decomposition method.

2 Experimental

Fe and Nb codoped STO samples (including 1% ^{57}Fe) were prepared by using a complex formation and thermal decomposition method. Each chemical of 0.1 M $SrCO_3$, 0.1 M Ti $(OCH(CH_3)_2)_4$, 0.01 M ^{57}Fe metal and 0.01 M Nb_2O_5 was dissolved in an acidic solution containing citric acid. The citric acid solutions were prepared by mixing each solution in a certain nominal mole ratio. Furthermore, the mixed solutions after adding ethylene glycol were stirred at around 90 °C, and heated at 500 °C for 2 h. After that, the samples were crushed and annealed at 1000 °C for 4 h. $SrTi_{1-x-y}Fe_xNb_yO_3$ doped with x = 0.005, 0.01, 0.02, 0.04 and y = 0.05 were characterized by ^{57}Fe Mössbauer spectrometry, X-ray diffraction (XRD: non-monochromatic Cu Kα X-ray radiation), and vibration sample magnetometer (VSM). Mössbauer spectra were calibrated with α-Fe and analysed by using MossWinn program.

3 Results and discussion

The XRD of STO samples with the 0.5% to 4% Fe and 5% Nb are shown in Fig. 1. All the XRD patterns for samples prepared at 1000 °C resemble the spectrum of pure STO having the cubic perovskite structure, where the adjacent splitting peaks with the intensities of 2:1 can be assignable to respective diffractions from $K\alpha_1$ and $K\alpha_2$ X-rays. If the cubic phase of STO deformed to a tetragonal phase by doping, some peaks should split additionally to be multiplets. However, we could not find any splitting in the peaks except for the $K\alpha_1$ and $K\alpha_2$ X-ray diffractions, confirming the cubic crystal structure of the prepared samples. The dopants are substituted in Ti sites of the cubic crystal since the impurity peaks were not significantly detected after annealing at 1000 °C. The 1% Fe and 5% Nb codoped STO perovskite showed the smallest lattice constant of $a = 3.907$ Å among the other samples prepared (3.907 Å $\leqq a \leqq$ 3.917 Å). The structural deformation accompanied with doping into the perovskite was analyzed using linewidths based on respective $K\alpha_1$ peak, that is Williamson-Hall plots as follows: $\beta\cos\theta = X + Y\sin\theta$, where β denotes the linewidth ($\Delta 2\theta$) as full width at half maximum, X and Y are the factors expressed as size effect and deformation effect, respectively. With decreasing concentration of Fe dopant, the gradient (Y) in the $\beta\cos\theta$ vs $\sin\theta$ plots increased monotonically as shown in Fig. 2. The result indicates that lower Fe doping induces deformation of the cubic crystal structure for the doped STO samples, which is accountable for the following reasons. Assuming that both Nb^{5+} and Fe^{3+} ions are substituted at Ti^{4+} ion sites in STO perovskites, the difference between doping rates of Nb and Fe ions is considered to induce the deformation of perovskite cubic crystals since these materials are charge-neutralized. The ionic radius is 0.67 Å for Fe^{3+} (coordination number: 6), and 0.69 Å for Nb^{5+} (6), whereas 0.64 Å for Ti^{4+} (6). If STO is a perfect crystal without oxygen defects, the lattice parameters should increase since the ionic radii of Fe^{3+} and Nb^{5+} are larger than that of Ti^{4+}. However, the lattice parameters of all doped perovskites became small as compared with that of STO without dopants (3.917 Å). Therefore, it is considered that since some oxygen defects are included in these perovskite oxides, the larger difference between Fe and Nb dopants, that is, less Fe dopants as compared with 5% Nb, affects relatively large deformation.

Magnetic properties of STO perovskites measured by VSM showed ferromagnetic and paramagnetic behaviors as shown in Fig. 3. The 1% Fe + 5% Nb codoped sample with the smallest lattice constant showed the largest ferromagnetism among these samples. The paramagnetic fraction increased with increase of Fe concentration. A larger ferromagnetic hysteresis was recognized for 1% Fe doping sample than for 0.5% Fe doping one although larger deformation of cubic perovskites was obtained for lower Fe doping rates. It is considered the reason why the Fe magnetic ions interact more easily with each other at nearest sites in 1% Fe doping STO than in 0.5% Fe doping one since 1% Fe doped STO has twice as large as concentration of Fe and the shortest lattice constant. It is furthermore considered from the shortest lattice constant that a small number of Fe dopants may occupy not only the Ti sites but also the Sr sites.

As shown in Fig. 4, Mössbauer spectra consist of paramagnetic doublet and magnetic relaxation components except the 4% Fe doped STO perovskite, the Mössbauer spectrum of which was analyzed as two paramagnetic doublets. From the isomer shift (*IS*) values (0.2–0.4 mm/s) of both components, it is found that ^{57}Fe species in the prepared samples exist as high spin Fe^{3+} ions with less oxygen coordination number. The magnetic relaxation peak

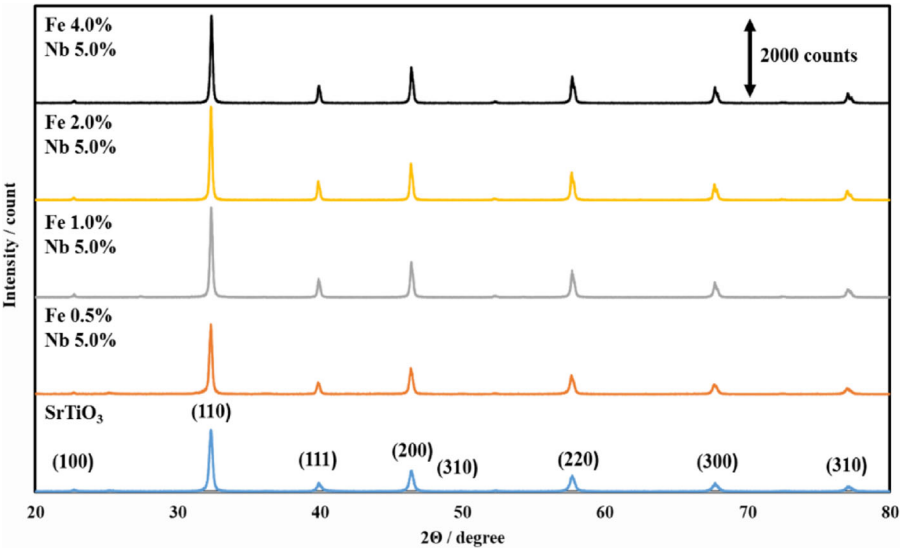

Fig. 1 X-ray diffraction patterns of Fe and Nb codoped $SrTiO_3$ annealed at 1000 °C for 4 h

appears stronger as the doped Fe concentration becomes lower. The result rules out the precipitation of magnetic iron clusters in synthesis processes. It is considered that the dilute

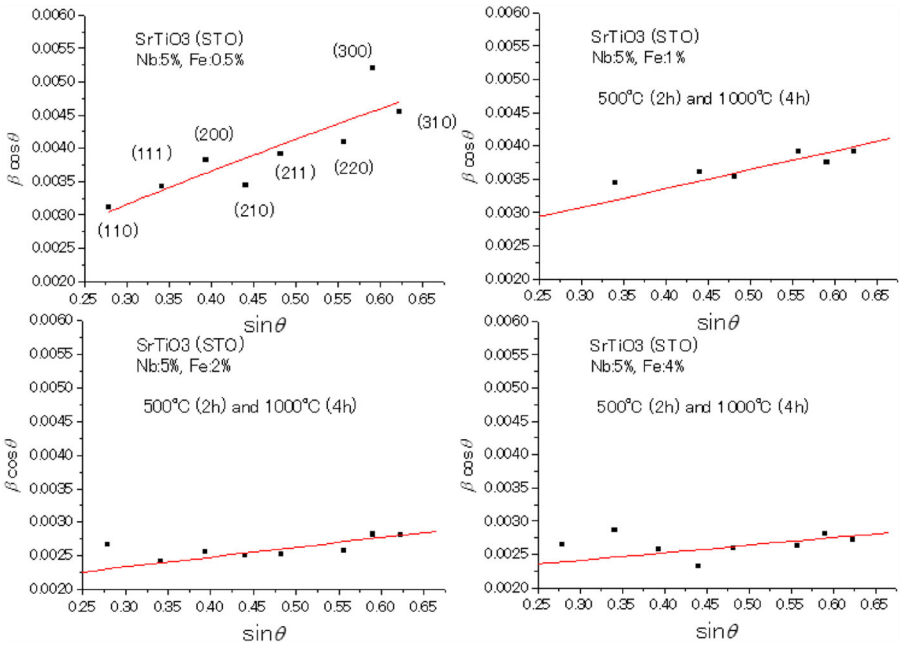

Fig. 2 Williamson-Hall plots obtained from XRD peaks of $SrTi_{0.95-x}Nb_{0.05}Fe_xO_{3-\delta}$(x = 0.005, 0.01, 0.02 and 0.04)

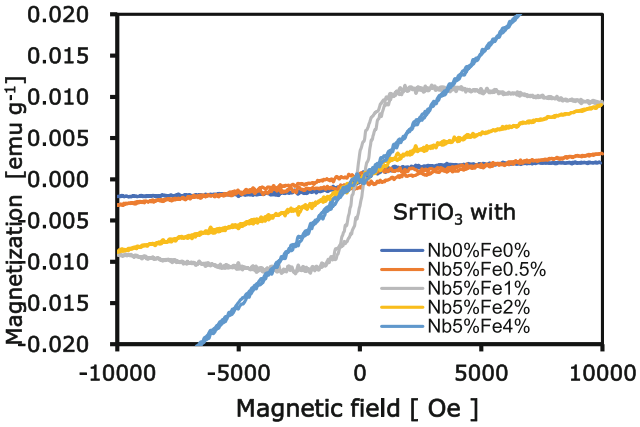

Fig. 3 RT magnetization curves of STO doped with various % Fe and 5% Nb

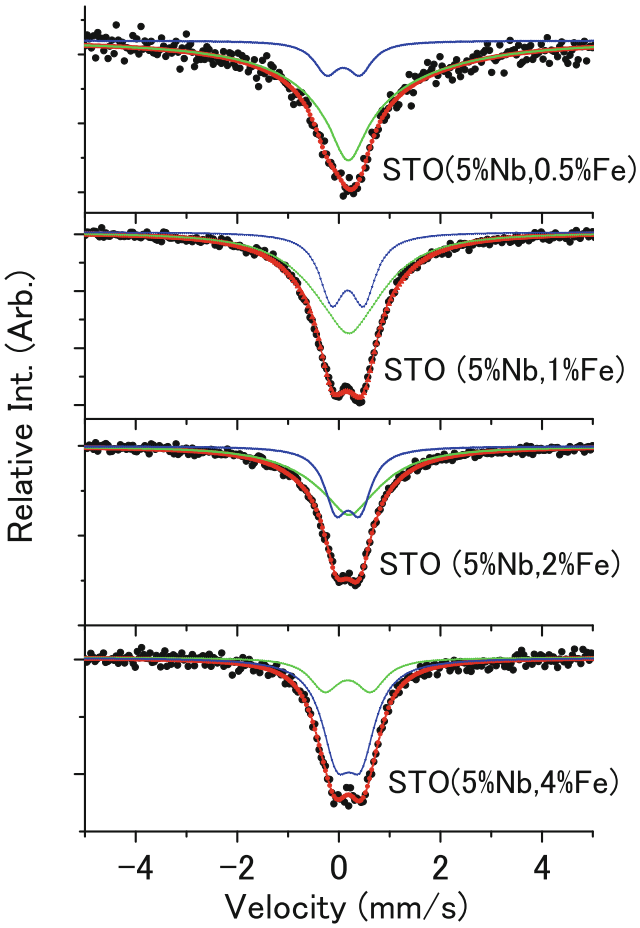

Fig. 4 RT Mössbauer spectra $SrTi_{0.95-x}Nb_{0.05}Fe_xO_{3-\delta}$ (x = 0.005, 0.01, 0.002, and 0.004)

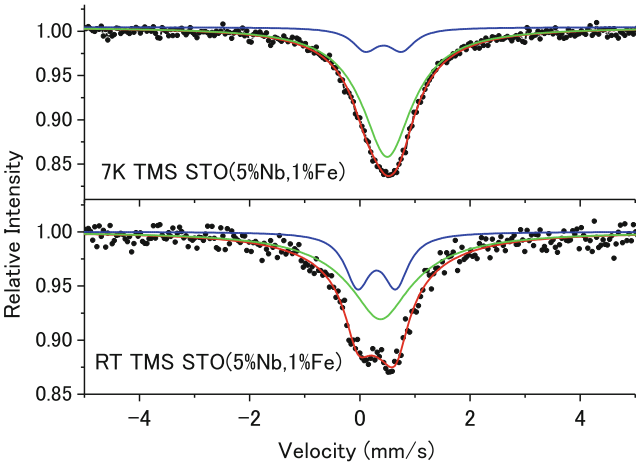

Fig. 5 RT and 7 K "transmission" Mössbauer spectra "(TMS)" of $SrTi_{0.94}Nb_{0.05}Fe_{0.01}O_{3-\delta}$, analyzed with the same linewidth of doublet in both spectra

magnetism in this system is related with oxygen defects, which suggests the formation of polarons [11].

The Mössbauer spectra of 1% Fe doped STO (Nb), measured at room temperature and low temperature of 7 K, are shown in Fig. 5. The increase of magnetic relaxation component without broadening on cooling was observed in addition to an increase of *IS* due to temperature dependence (secondary Doppler shift). It is clear that the ratios of doublet and magnetic relaxation components are very different between RT and low temperature Mössbauer spectra. Thus, the dilute magnetism of STO is different from conventional ferromagnetic materials in temperature dependence. The temperature dependency of this system should be further studied.

4 Conclusion

Cubic perovskite oxides, STO doped with 5% Nb and 0.5% to 4% Fe, were prepared by a complex synthesis and thermal decomposition method, and characterized by XRD, VSM, and ^{57}Fe Mossbauer spectrometry. In the Mössbauer spectra, a ferromagnetic relaxation peak was observed as a major component in lower Fe doped STO perovskites, while a paramagnetic component became dominant for higher Fe doping samples. It is concluded that diluted magnetism in this system is related mainly with the deformation of the cubic structure due to the different amounts between Fe and Nb dopants.

References

1. Nomura, K.: Croat. Chem. Acta **88**, 579–590 (2015)
2. Prajapati, B., Kumar, S., Kumar, M., Chatterjee, S., Ghosh, A.K.: J. Mater. Chem. C **5**, 4257–4267 (2017)
3. Beltrán, J.J., Barrero, C.A., Punnoose, A.: J. Phys. Chem. C **118**, 13203–13217 (2014)
4. Kumar, A.S., Suresh, P., Kumar, M.M., Srikanth, H., Post, M.L., Sahner, K., Moos, R., Srinath, S.: J. Phys.: Conf. Ser. **200**, 1–4 (2010)

5. Karaphun, A., Hunpratub, S., Swatsitang, E.: Microelectron. Eng. **126**, 42–48 (2014)
6. Şale, A.G., Kazan, S., Gatiiatova, J.I., Valeev, V.F., Khaibullin, R.I., Mikailzade, F.A.: Mater. Res. Bull. **48**, 2861–2864 (2013)
7. Karczewski, J., Riegel, B., Gazda, M., Jasinski, P., Kusz, B.: J. Electroceram. **24**, 326–330 (2010)
8. Zhao, T., Lu, H., Chen, F., Dai, S., Yang, G., Che, Z.: J. Crys. Growth **212**, 451–455 (2000)
9. Modak, B., Ghosh, S.K.: J. Phys. Chem. C **119**, 23503–23514 (2015)
10. Coey, J.M.D., Venkatesanan, M., Stamenov, P.: J. Phys. Cond. Matter. **28**, 485001 (2016)
11. Coey, J.M.D., Venkatesan, M., Fitzgerald, C.B.: Nature Mater. **4**, 173 (2005)